Huijun Li
School of Energy Power and Mechanical Engineering,
North China Electric Power University,
Box 27, No. 619 Yonghua North Road,
Baoding 071003, China
e-mail: hj_li009@sina.com

Wenping Peng
School of Energy Power and Mechanical Engineering,
North China Electric Power University,
Box 27, No. 619 Yonghua North Road,
Baoding 071003, China
e-mail: wenpingpeng@gmail.com

Yingguang Liu
School of Energy Power and Mechanical Engineering,
North China Electric Power University,
Box 27, No. 619 Yonghua North Road,
Baoding 071003, China
e-mail: yingguang266@126.com

Chao Ma
School of Energy Power and Mechanical Engineering,
North China Electric Power University,
Box 27, No. 619 Yonghua North Road,
Baoding 071003, China
e-mail: 569242650@qq.com

Effect of Tube Geometry and Curvature on Film Condensation in the Presence of a Noncondensable Gas

Based on the double boundary layer theory, a generalized mathematical model was developed to study the distributions of gas film, liquid film, and heat transfer coefficient along the tube surface with different geometries and curvatures for film condensation in the presence of a noncondensable gas. The results show that: (i) for tubes with the same geometry, gas film thickness, and liquid film thickness near the top of the tube decrease with the increasing of curvature and the heat transfer rate increases with it. (ii) For tubes with different geometries, one need to take into account all factors to compare their overall heat transfer rate including gas film thickness, liquid film thickness and the separating area. Besides, the mechanism of the drainage and separation of gas film and liquid film was analyzed in detail. One can make a conclusion that for free convection, gas film never separate since parameter A is always positive, whereas liquid film can separate if parameter B becomes negative. The separating angle of liquid film decreases with the increasing of curvature. [DOI: 10.1115/1.4028345]

Keywords: condensation heat transfer, gas film thickness, liquid film thickness, tube geometry, noncondensable gases

1 Introduction

The phenomena of film condensation in the presence of a noncondensable gas widely exist in the industrial heat transfer equipments. Any improvement in the performance of such equipments can bring considerable economic benefit. The vapor–gas condensation process involves thermal resistances due to the noncondensable gases and the condensate liquid film. Gas phase heat resistance is the dominant factor that reduces the efficiency of overall condensation heat transfer. The tube geometry not only impacts flow field but also affects various parameters associated with gas and liquid films. The optimum tube geometry is therefore beneficial to reduce involved thermal resistances and improve the performance of heat exchange equipments. Many researchers have studied the influence of tube geometry on condensation heat transfer. A brief discussion on some significant contributions follows. Yang and Hsu [1] theoretically compared the condensation heat transfer characteristics outside a circular tube with that on an elliptical tube. It was found that the elliptical tube has better performance of condensation heat transfer than the circular one. Memory et al. [2] studied free and forced convection laminar film condensation on the horizontal elliptical tube in a pure saturated vapor. For free convection, an elliptical tube with the major axis vertical shows an improvement of near 11% in the mean heat transfer coefficient compared to a circular tube in equivalent surface area. For force convection, under similar conditions and with the same pressure drop, the heat transfer performance increases up to 16%. Chang and Yeh [3] investigated the condensation heat transfer on a horizontal elliptical tube in stationary saturated vapor with wall suction. It was found that the tube curvature has a significant influence on the mean Nusselt number. Li [4] experimentally studied the heat transfer characteristics of flue gas condensation over the droplet-shaped tube bundle. Droplet-shaped tube bundle shows an improvement of near 7% in the heat transfer efficiency compared to circular tube bundle in equivalent surface area. What's more, as demonstrated by Som and Chakraborty [5] and Mukhopadhyay et al. [6], it was investigated about the condensation heat transfer performance of vapor–gas mixture outside a tube with three different geometries for free convection. An enhancement in the overall heat transfer rate for both elliptic and spiral surfaces has been observed compared to an equivalent circular tube surface. This is attributed to the combined effect of gravity and pressure gradient driven by surface tension in the direction of the condensate flow. However, all of them did not calculate gas film thickness and explain at length how tube geometry and its curvature affect the drainage and separation of gas and liquid films. Based on the double boundary layer theory, a generalized mathematical treatment is therefore established to investigate the distributions of gas film, liquid film, and heat transfer coefficient along a horizontal tube surface with different geometries and curvatures for film condensation in the presence of a noncondensable gas.

2 Geometric Conditions

Three kinds of tube geometry are chosen to be studied, including the circular tube, the elliptical tube and the equiangular spiral tube. For an elliptical tube, its major axis is aligned with the direction of gravity. For an equiangular spiral tube, the portion bounded by $\tan^{-1} m \le \theta \le \pi/2 + \beta$ is regarded as the half of the tube surface, and chord AB is the axis of symmetry of the equiangular spiral tube, as shown in Fig. 1. An elliptical tube with $e = 0$ becomes the circular one and an equiangular spiral tube with $m = 0$ also does.

As demonstrated by Mukhopadhyay et al. [6], the relational expression of β and m for an equiangular spiral tube is

Contributed by the Heat Transfer Division of ASME for publication in the Journal of Thermal Science and Engineering Applications. Manuscript received January 12, 2014; final manuscript received June 17, 2014; published online September 16, 2014. Assoc. Editor: Mehmet Arik.

Copyright © 2015 by ASME

Downloaded From: https://thermalscienceapplication.asmedigitalcollection.asme.org on 06/29/2019 Terms of Use: http://www.asme.org/about-asme/terms-of-use

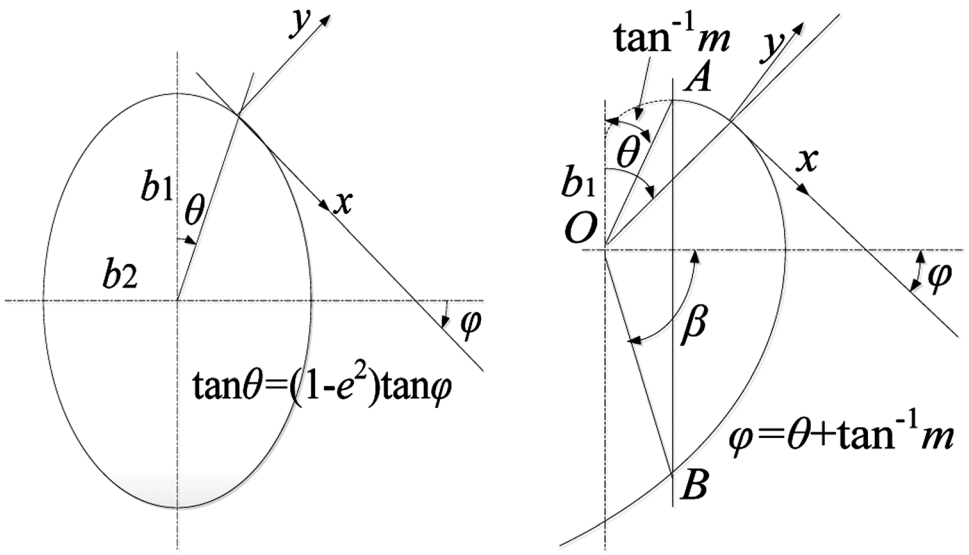

(a) (b)

Fig. 1 Condensing surfaces with different geometries. (*a*) A horizontal ellipse and (*b*) an equiangular spiral curve.

$$\cos\beta = \frac{\exp(m\tan^{-1}m)\sin(\tan^{-1}m)}{\exp[m(\pi/2+\beta)]} \tag{1}$$

For an elliptical tube, x and φ are related as demonstrated by Chang and Yeh [3], namely

$$dx = \frac{b_1(1-e^2)}{\left(1-e^2\sin^2\phi\right)^{3/2}}d\varphi \tag{2}$$

And for an equiangular spiral tube, x and θ are related as demonstrated by Mukhopadhyay et al. [6], namely

$$dx = b_1\exp(m\theta)\sqrt{1+m^2}d\theta \tag{3}$$

3 Physical Model

The process of vapor–gas film condensation heat transfer is very complex. For simplifying the situation, some basic assumptions are set as: (1) total pressure in gas film is constant; (2) bulk temperature and bulk mass concentration of the noncondensable gas are kept unchanged along the tube surface; (3) condensation only occurs at the gas–liquid interface; (4) all the physical process are steady in gas and liquid films; (5) flow in gas and liquid films is laminar; (6) thickness of gas film and liquid film are far smaller than the tube diameter; (7) pressure gradient along the gas–liquid interface is only driven by surface tension of the condensate; (8) inertia force is ignored in the momentum conservation equation of liquid film; (9) convective term is also ignored in the energy conservation equation of liquid film; (10) interface thermal resistance is negligible, and interface temperature is equivalent to the saturation temperature corresponding with the partial pressure of vapor there; (11) the temperature on the tube surface is constant in the circumference of the tube; (12) vapor of mixture is in a saturated state; (13) the noncondensable gas, the vapor, and the vapor–gas mixture are all treated as ideal gases; and (14) the condensate surface is impermeable to the noncondensable gas.

Taking the circular one as an example, its physical model and coordinate system are shown in Fig. 2. A film due to the condensate forms along the tube surface if condensation occurs and keeps steady. Besides, there is a film due to the noncondensable gas between the condensate film and the bulk. What's more, there are a boundary layer of heat transfer and a boundary layer of momentum in gas film, as shown in Fig. 2. δ_u is approximately equal to $Sc^{1/3}\delta_m$ and δ_t does $Le^{1/3}\delta_m$ as demonstrated by Yang and Tao [7]. In the direction perpendicular to the tube surface, the position in liquid film is expressed by y_l $(0<y_l<\delta_l)$ and that in gas film does by y $(0<y<\delta_m)$, in order to simplifying the calculation.

4 Mathematical Model

4.1 Governing Equations and Boundary Conditions. According to the Prandtl boundary layer theory and the assumptions above, the momentum conservation equation in liquid film can be simplified as

$$\mu_l\frac{\partial^2 u_l}{\partial y_l^2} + (\rho_l-\rho)g\sin\varphi - \frac{dp}{dx} = 0 \tag{4}$$

where the first term represents viscosity force, the second term the difference between gravity of the condensate and buoyancy force in the tangential direction of the tube surface, and the third term pressure gradient caused by surface tension.

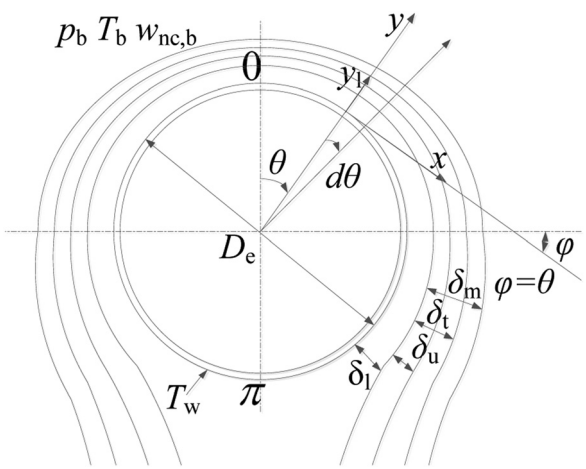

Fig. 2 Physical model and coordinate system of the circular one

Downloaded From: https://thermalscienceapplication.asmedigitalcollection.asme.org on 06/29/2019 Terms of Use: http://www.asme.org/about-asme/terms-of-use

According to the Prandtl boundary layer theory and the assumptions above, the momentum conservation equation in gas film can be simplified as

$$\nu\frac{\partial u}{\partial y}=\upsilon\frac{\partial^2 u}{\partial y^2}+g\sin\varphi\left\{1-\frac{T[M_{\rm nc}-(M_{\rm nc}-M_v)w_{\rm nc}]}{T_b\left[M_{\rm nc}-(M_{\rm nc}-M_v)w_{\rm nc,b}\right]}\right\} \quad (5)$$

where the term on the left side of represents inertial force, the first term on the right side viscosity force, and the second term the difference between gravity of vapor–gas mixture and buoyancy force in the tangential direction of the tube surface.

According to the Prandtl boundary layer theory and the assumptions above, the energy conservation equation in gas film can be simplified as

$$v\frac{\partial \mathrm{T}}{\partial y}=a\frac{\partial^2 T}{\partial y^2}+D\frac{c_{\rm pnc}-c_{\rm pv}}{c_p}\frac{\partial}{\partial y}\left(T\frac{\partial w_{\rm nc}}{\partial y}\right) \quad (6)$$

where the second term on the right side is negligible for free convection.

According to the Prandtl boundary layer theory and the assumptions above, the noncondensable gas diffusion equation in gas film can be simplified as

$$\nu\frac{\partial w_{\rm nc}}{\partial y}=D\frac{\partial^2 w_{\rm nc}}{\partial y^2} \quad (7)$$

The boundary conditions for this situation are as follows:

At the tube surface ($y_{\rm l}=0$)

$$u_{\rm l}=0,\quad T_{\rm l}=T_{\rm w} \quad (8)$$

At the edge of boundary layer of mixture momentum ($y=\delta_{\rm u}$)

$$u=0 \quad (9)$$

At the edge of boundary layer of mixture heat transfer ($y=\delta_{\rm t}$)

$$T=T_{\rm b} \quad (10)$$

At the edge of boundary layer of noncondensable gas diffusion or gas film($y=\delta_{\rm m}$)

$$w_{\rm nc}=w_{\rm nc,b} \quad (11)$$

At the gas–liquid interface ($y_{\rm l}=\delta_{\rm l}$ or $y=0$)

$$u=u_{\rm l},\quad \mu_{\rm l}\frac{\partial u_{\rm l}}{\partial y_{\rm l}}=\mu\frac{\partial u}{\partial y}=0 \quad (12)$$

$$T=T_i \quad (13)$$

$$w_{\rm nc}=w_{\rm nc,i} \quad (14)$$

$$m_{\rm c}=\rho_{\rm l}\frac{d}{dx}\int_0^{\delta_{\rm l}}u_{\rm l}dy_{\rm l} \quad (15)$$

$$k_{\rm l}\frac{T_{\rm i}-T_{\rm w}}{\delta_{\rm l}}=h'_{\rm fg}m_{\rm c}+q_{\rm s} \quad (16)$$

4.2 Analytic Expressions of Some Quantities. According to Eq. (14), the velocity along y direction in gas film can be expressed as demonstrated by Lee and Kim [8], namely

$$v=\frac{D}{w_{\rm nc}}\cdot\frac{\partial w_{\rm nc}}{\partial y} \quad (17)$$

By combining Eqs. ((7), (11), (14), and (17)), one can solve the equation of noncondensable gas diffusion as

$$w_{\rm nc}=w_{\rm nc,i}\exp\left[\frac{y}{\delta_{\rm m}}\ln\left(\frac{w_{\rm nc,b}}{w_{\rm nc,i}}\right)\right] \quad (18)$$

By inserting Eq. (18) into Eq. (17), the velocity along y direction in gas film can be given as

$$\nu=\frac{D}{\delta_{\rm m}}\ln\frac{w_{\rm nc,b}}{w_{\rm nc,i}} \quad (19)$$

Since vapor mass flux is driven by diffusion and convection, the condensate mass flux can be obtained as demonstrated by Rosa et al. [9], namely

$$m_{\rm c}=\frac{\rho D}{\delta_{\rm m}}\ln\frac{w_{\rm nc,i}}{w_{\rm nc,b}} \quad (20)$$

By combining Eqs. ((6), (10), (13), and (19)), one can solve the equation of heat transfer in gas film as follows:

$$T=(T_{\rm b}-T_i)\frac{\exp\left(\dfrac{y}{{\rm Le}\delta_{\rm m}}\ln\dfrac{w_{\rm nc,b}}{w_{\rm nc,i}}\right)-1}{\exp\left[{\rm Le}^{-2/3}\ln\dfrac{w_{\rm nc,b}}{w_{\rm nc,i}}\right]-1}+T_i \quad (21)$$

The heat flux due to convection in gas film can be deduced using Eq. (21) as

$$q_{\rm s}=k(T_{\rm b}-T_i)\frac{1}{{\rm Le}\delta_{\rm m}}\frac{1}{\exp\left({\rm Le}^{-2/3}\ln\dfrac{w_{\rm nc,b}}{w_{\rm nc,i}}\right)-1}\ln\frac{w_{\rm nc,b}}{w_{\rm nc,i}} \quad (22)$$

By combining Eqs. ((5), (9), (12), and (19)), one can solve the momentum equation in gas film as follows:

$$u=\frac{A}{\nu}\left[y-{\rm Sc}^{1/3}\delta_{\rm m}-\frac{\upsilon}{v}\left(e^{\frac{v}{\upsilon}y}-e^{\frac{v}{\upsilon}{\rm Sc}^{1/3}\delta_{\rm m}}\right)\right] \quad (23)$$

where $A=g(\sin\varphi-[\rho_b/\rho]\sin\varphi)$.

Parameter A in Eq. (23) represents the influence of gravity of mixture and pressure gradient driven by buoyancy on the drainage of gas film. The first term in parameter A denotes the effect of tube geometry and curvature on the component of gravity in the tangential direction of the tube surface, and the second term in parameter A is the ratio of pressure gradient due to buoyancy to gravity of mixture, reflecting the influence of tube geometry, and curvature on pressure gradient.

By combining Eqs. ((4), (8), and (12)), one can solve the momentum equation in liquid film as

$$u_{\rm l}=\frac{B}{\mu_{\rm l}}\left(y_{\rm l}\delta_{\rm l}-\frac{1}{2}y_{\rm l}^2\right) \quad (24)$$

where $B=(\rho_{\rm l}-\rho)g[\sin\varphi-((dp/dx)/(\rho_{\rm l}-\rho)g)]$.

Parameter B in Eq. (24) represents the influence of gravity of the condensate and pressure gradient driven by surface tension on the drainage of liquid film. The first term in parameter B denotes the effect of tube geometry and curvature on the component of gravity in the tangential direction of the tube surface, and the second term in parameter B is the ratio of pressure gradient due to surface tension to gravity of the condensate, reflecting the influence of tube geometry and curvature on pressure gradient.

Considering that total heat flux is equivalent to heat conduction flux in liquid film, local heat transfer coefficient can be given as

$$h=\frac{k_{\rm l}}{\delta_{\rm l}}\cdot\frac{T_{\rm i}-T_{\rm w}}{T_{\rm b}-T_{\rm w}} \quad (25)$$

Downloaded From: https://thermalscienceapplication.asmedigitalcollection.asme.org on 06/29/2019 Terms of Use: http://www.asme.org/about-asme/terms-of-use

Table 1 Calculation parameters

Parameters	Values
Total pressure, p_b (Pa)	101,325
Air mass fraction, $w_{nc,b}$ (%)	0.1–50
Tube surface temperature, T_w (K)	353
Eccentricity, e	0–0.9
Parametric constant, m	0–2
Equivalent diameter, D_e (m)	0.0254

4.3 Relationships of Gas Film Thickness and Liquid Film Thickness. Gas film thickness and liquid film thickness can be obtained only if interface temperature is solved. There are three unknown variables, including gas film thickness, liquid film thickness and interface temperature. So it is required three irrelevant equations to get interface temperature.

Insert Eq. (24) into Eq. (15) and combine Eqs. (15) and (20), and the first relational expression can be derived as

$$\frac{1}{3\upsilon_l}\left(\frac{dB}{dx}\delta_l^3 + 3B\delta_l^2\frac{d\delta_l}{dx}\right) = \frac{\rho D}{\delta_m}\ln\frac{w_{nc,i}}{w_{nc,b}} \tag{26}$$

Substitute Eqs. (23) and (24) into the first term in Eq. (12), and the second relational expression can be obtained as:

$$\frac{A}{v}\left[-\mathrm{Sc}^{1/3}\delta_m - \frac{\upsilon}{v}\left(1 - e^{\frac{v}{\upsilon}\mathrm{Sc}^{1/3}\delta_m}\right)\right] = \frac{B}{2\mu_l}\delta_l^2 \tag{27}$$

Bring Eqs. ((20) and (22)) into Eq. (16), and the third relational expression can be written as

$$k_l\frac{T_i - T_w}{\delta_l} = \frac{\ln\frac{w_{nc,i}}{w_{nc,b}}}{\delta_m} \times \left[\rho D h'_{fg} + k(T_b - T_i)\cdot\frac{1}{\mathrm{Le}}\cdot\frac{1}{1 - \exp\left(\mathrm{Le}^{-2/3}\ln\frac{w_{nc,b}}{w_{nc,i}}\right)}\right] \tag{28}$$

For an elliptical tube, the pressure gradient due to surface tension can be derived as demonstrated by Chang and Yeh [3], namely

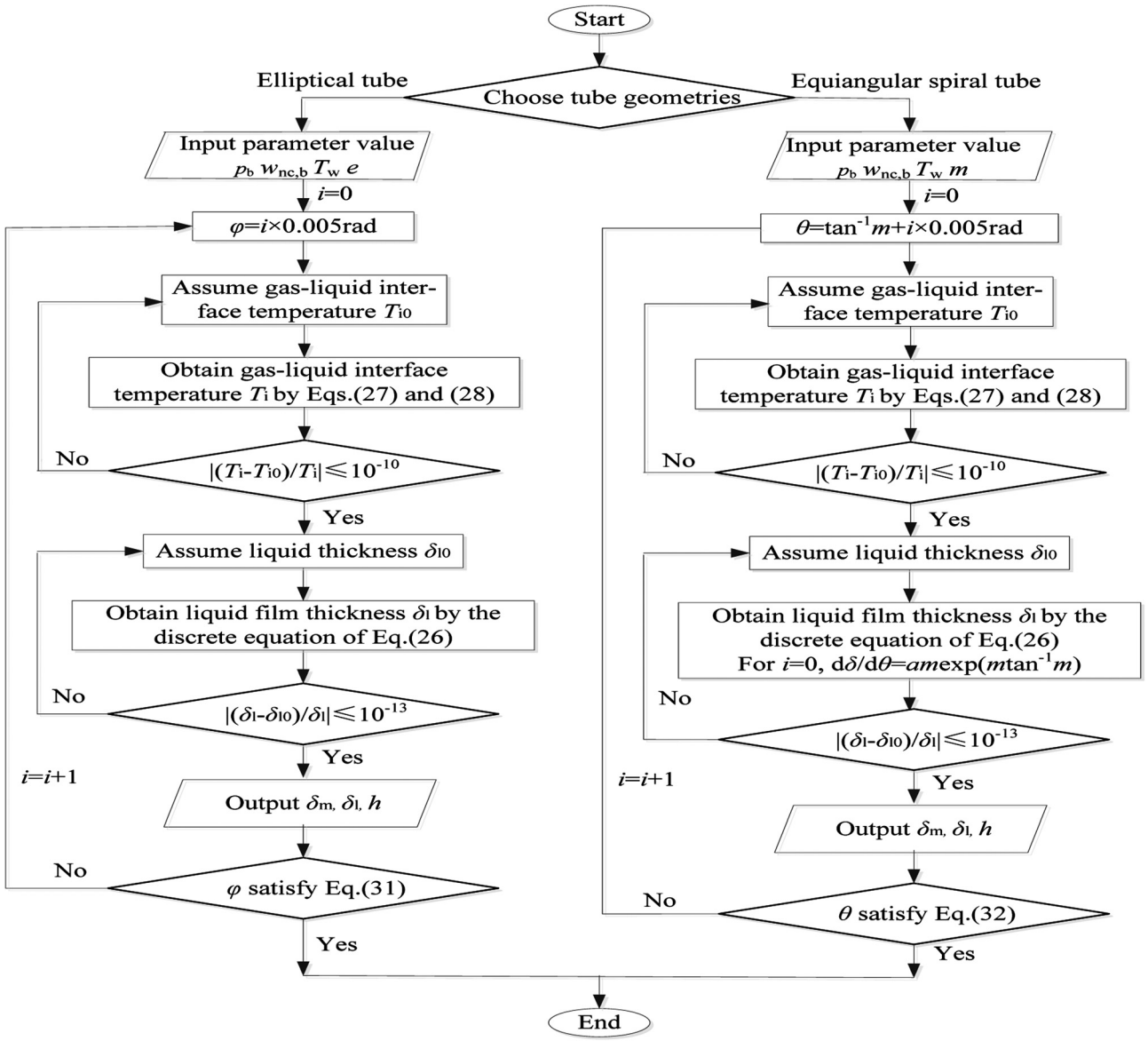

Fig. 3 Calculation scheme flowchart

Downloaded From: https://thermalscienceapplication.asmedigitalcollection.asme.org on 06/29/2019 Terms of Use: http://www.asme.org/about-asme/terms-of-use

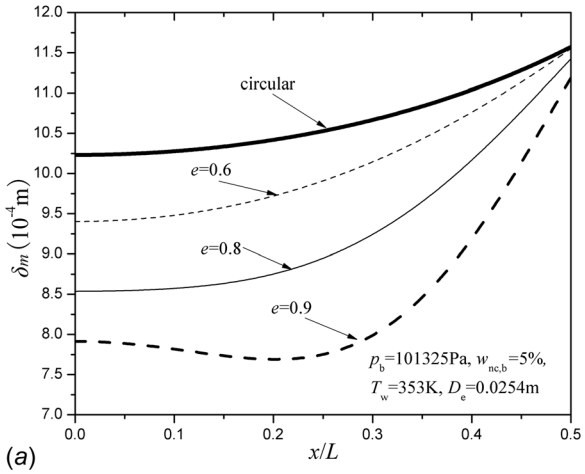

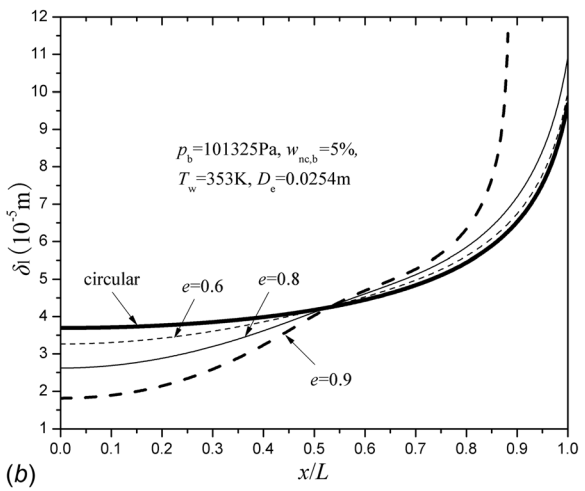

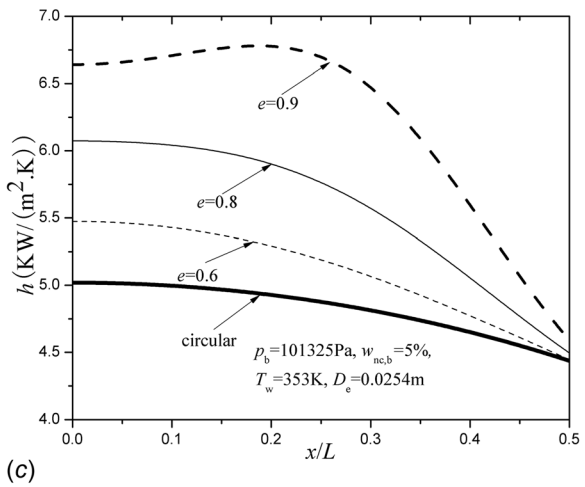

Fig. 4 The distributions of gas film, liquid film, and heat transfer coefficient along the tube surface with different *e* for an elliptical tube. (*a*) Gas film thickness, (*b*) liquid film thickness, and (*c*) heat transfer coefficient.

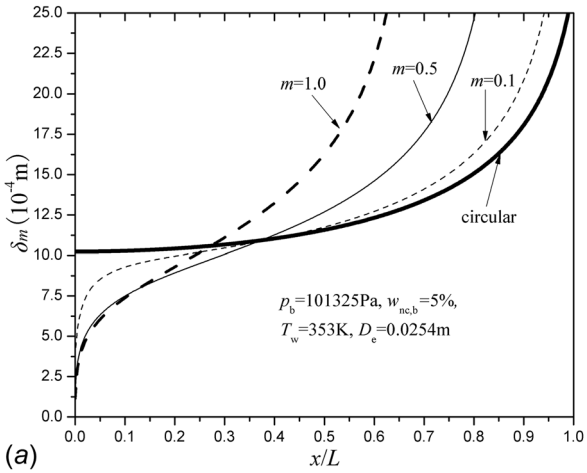

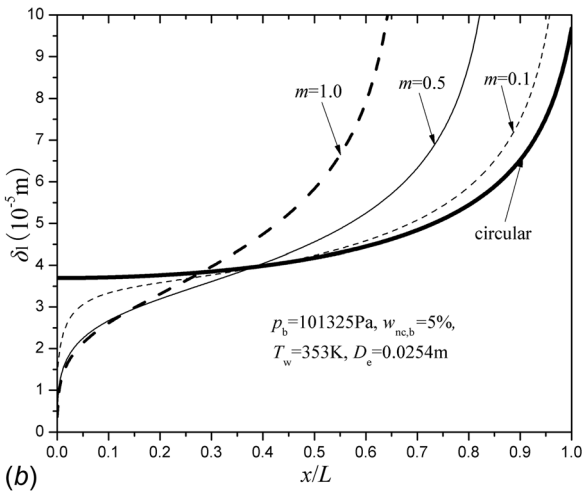

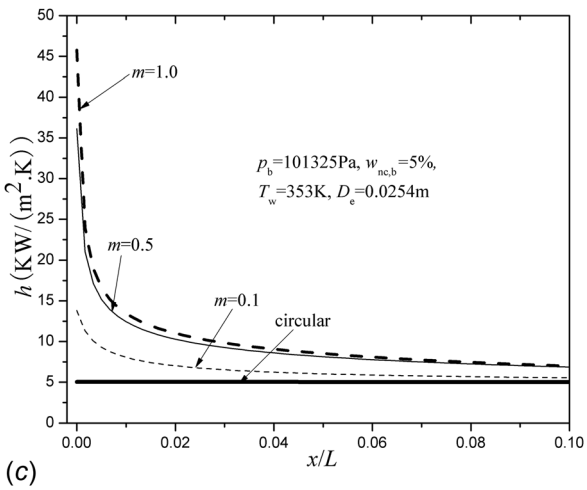

Fig. 5 The distributions of gas film, liquid film, and heat transfer coefficient along the tube surface with different *m* for an equiangular spiral tube. (*a*) Gas film thickness, (*b*) liquid film thickness, and (*c*) heat transfer coefficient.

$$\frac{\mathrm{d}p}{\mathrm{d}x} = -\frac{\sigma}{b_1^2}\frac{3e^2}{2}\left(\frac{1-e^2\sin^2\varphi}{1-e^2}\right)^2 \sin 2\varphi \tag{29}$$

For an equiangular spiral tube, the pressure gradient due to surface tension can be expressed as Mukhopadhyay et al. [6], namely

$$\frac{\mathrm{d}p}{\mathrm{d}x} = -\frac{\sigma m \exp(-2m\theta)}{b_1^2(1+m^2)} \tag{30}$$

4.4 Liquid Film Separation. If velocity gradient in the y direction is negative, there is stagnation or backflow. Hence, liquid film separates in the condition of $\partial u_l/\partial y_l|_{yl=0} \le 0$ as demonstrated by Hsu and Yang [10]. For an elliptical tube, liquid film separation occurs if angle φ meets the expression which is as follows:

Downloaded From: https://thermalscienceapplication.asmedigitalcollection.asme.org on 06/29/2019 Terms of Use: http://www.asme.org/about-asme/terms-of-use

$$(\rho_l - \rho) g \sin\varphi + \frac{\sigma}{b_1^2}\frac{3e^2}{2}\left(\frac{1 - e^2\sin^2\varphi}{1 - e^2}\right)^2 \sin 2\varphi \le 0 \qquad (31)$$

By the same token, for an equiangular spiral tube, liquid film separation also occurs if angle θ meets the expression which is as follows:

$$(\rho_l - \rho) g \sin\left(\theta + \tan^{-1} m\right) + \frac{\sigma m \exp(-2m\theta)}{b_1^2(1 + m^2)} \le 0 \qquad (32)$$

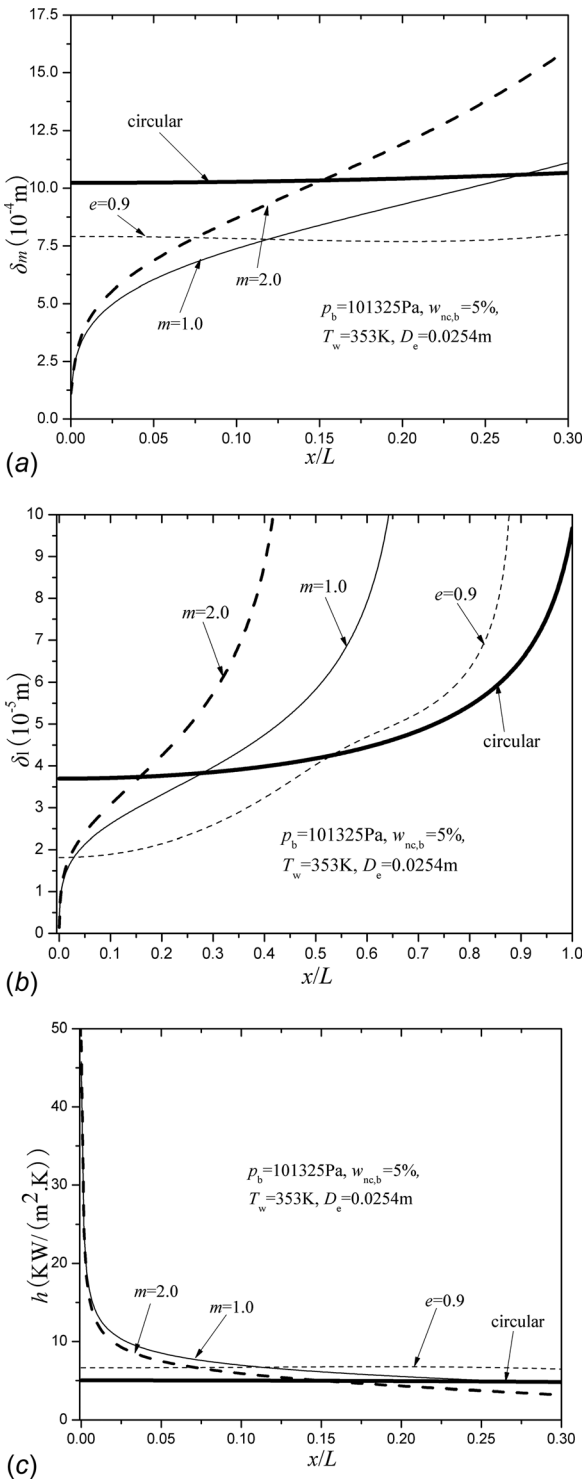

Fig. 6 The distributions of gas film, liquid film, and heat transfer coefficient along the tube surface for an equiangular spiral tube and an elliptical tube. (*a*) Gas film thickness, (*b*) liquid film thickness, and (*c*) heat transfer coefficient.

5 Calculation

5.1 Calculation Parameters. Choose calculation parameters for water vapor–air mixture as shown in Table 1.

5.2 Solving Process. The nonlinear equation about T_i can be obtained by combining Eqs. ((27) and (28)), and T_i can be solved by using the iteration method with the convergence accuracy of $|T_i - T_{i0}|/T_i \le 10^{-10}$. The differential term in Eq. (26) is discretized by using the finite difference method with the step size of 0.005 rad. Liquid film thickness can be solved through Eq. (26) by using the iteration method with the convergence accuracy of $|\delta_l - \delta_{l0}|/\delta_l \le 10^{-13}$. Gas film thickness can be obtained by substituting liquid film thickness and interface temperature into Eq. (28). If φ meets Eq. (31) or θ meets Eq. (32), it manifests that liquid film separates then calculation should be stopped. Solving process programmed by C++ language, is as shown in Fig. 3. In the data processing, the position in the x direction is expressed by dimensionless variable x/L.

6 Results and Discussion

6.1 Elliptical Tube. Gas film thickness and liquid film thickness increase along the tube surface and their gradient also does, approaching to infinite near the bottom of the tube or the separating point. Gas film thickness and liquid film thickness decrease with the increasing of e near the top of the tube, but they inversely do after x/L exceeds certain value, as shown in Figs. 4(*a*) and 4(*b*). Moreover, liquid film separates at $\varphi = 151.6$ deg for $e = 0.9$, as shown in Fig. 4(*b*). Heat transfer coefficient decreases along the tube surface and its gradient inversely does. Heat transfer coefficient increases with the increasing of e near the top of the tube, yet it inversely does after x/L exceeds certain value, as shown in Fig. 4(*c*). Condensation heat transfer can be greatly enhanced with liquid film separating. The overall heat transfer rate increases with the increasing of the curvature.

6.2 Equiangular Spiral Tube. Gas film thickness and liquid film thickness increase along the tube surface, and for tubes of $m > 0$, their gradient first decreases along the tube surface and afterwards increases along it. Gas film thickness and liquid film

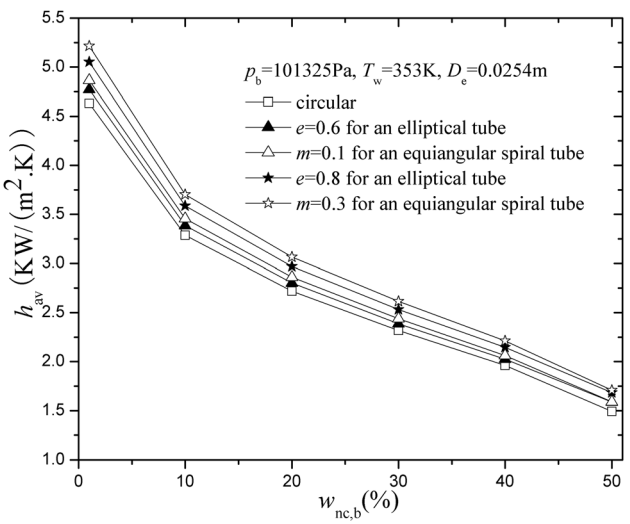

Fig. 7 The average heat transfer coefficients for different tube geometries and curvatures with bulk concentration of noncondensable gas in the condition of liquid film nonseparating

Downloaded From: https://thermalscienceapplication.asmedigitalcollection.asme.org on 06/29/2019 Terms of Use: http://www.asme.org/about-asme/terms-of-use

thickness decrease with the increasing of m near the top of the tube, but inversely does after x/L exceeds certain value, as shown in Figs. 5(*a*) and 5(*b*), Liquid film does not separate for tubes of $m=0$ and $m=0.1$, whereas it separates for tubes $m=0.5$ and $m=1.0$ and their separating angles are 153.3 deg and 134.8 deg, respectively, as shown in Fig. 5(*b*). Heat transfer coefficient decreases along the tube surface and its gradient also does. Heat transfer coefficient increases with the increasing of m near the top of the tube, but it inversely does after x/L exceeds certain value, as shown in Fig. 5(*c*). The separating angle decreases with the increasing of m if liquid film separates. The smaller is the separating angle of liquid film, the greater is the enhanced area of condensation heat transfer. The overall heat transfer rate increases with the increasing of the curvature.

6.3 Comparison of Elliptical Tube and Equiangular Spiral Tube. In equivalent surface area, gas film and liquid film formed outside both the elliptical tube and the equiangular spiral tube are thinner than those on the circular tube near the top of the tube and heat transfer coefficient there are greater than those on the circular one, as shown in Figs. 6(*a*)–6(*c*). For the equiangular spiral tube with $m=1.0$ or $m=2.0$, gas film and liquid film are thinner than those on the elliptical tube with $e=0.9$ near the top of the tube. Yet they become thicker than those on the elliptical tube with $e=0.9$ if x/L exceeds certain value, as shown in Figs. 6(*a*) and 6(*b*). And the heat transfer rate of the equiangular spiral tube with $m=1.0$ or $m=2.0$ is greater than that on the elliptical tube with $e=0.9$ near the top of the tube, whereas it becomes less than that on the elliptical tube with $e=0.9$ if x/L exceeds certain value, as shown in Fig. 6(*c*). The separating area of liquid film of the equiangular spiral tube with $m=1.0$ or $m=2.0$ is greater than that of the elliptical tube with $e=0.9$, as shown in Fig. 6(*b*). Therefore, whose heat transfer performance is better for the elliptical tube and the equiangular spiral tube needs to comprehensively consider all factors such as gas film thickness, liquid film thickness, the separating area, and so on. For the equiangular spiral tube with $m=1.0$ or $m=2.0$, its overall heat transfer rate is greater than that of the elliptical tube with $e=0.9$.

For tubes without liquid film separating in equivalent surface area, the decreasing sequence of the overall heat transfer rate is $m=0.3>e=0.8>m=0.1>e=0.6>$ circular ($e=0$ or $m=0$), as shown in Fig. 7.

7 Mechanism of the Drainage and Separation of Gas Film and Liquid Film

For tubes with the same geometry in equivalent surface area, $\sin\varphi$, and pressure gradient due to surface tension increase with the curvature increased, so the discharge capacity of gas film and

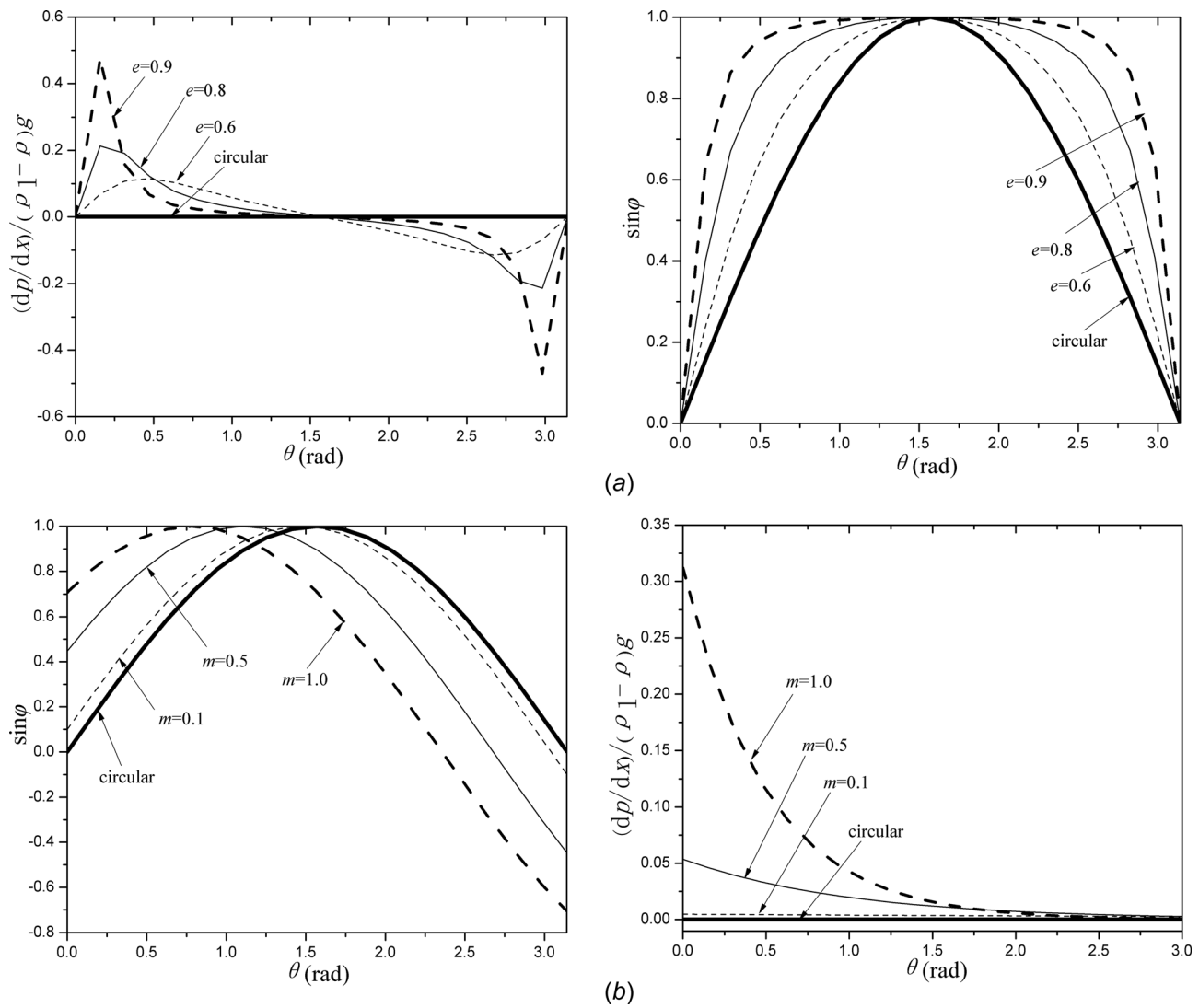

Fig. 8 The distributions of the parameters related to the discharge and separation along the tube surface (*a*) for an elliptical tube and (*b*) for an equiangular spiral tube

Downloaded From: https://thermalscienceapplication.asmedigitalcollection.asme.org on 06/29/2019 Terms of Use: http://www.asme.org/about-asme/terms-of-use

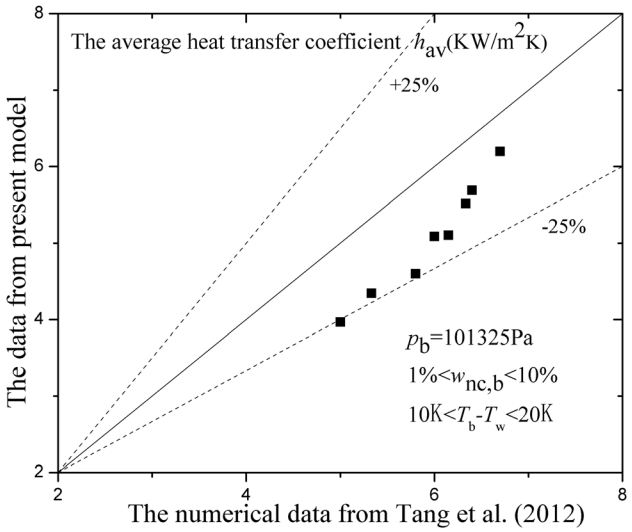

Fig. 9 Comparison of average heat transfer coefficient between the present model and the data from Tang et al. [11] for a circular tube

liquid film increases with the curvature increased, as shown in Fig. 8. This explains the reason why for tubes with the same geometry, gas film thickness, and liquid film thickness decrease with the increasing of the curvature.

Since parameter A is always positive for free convection, gas film cannot separate. For an elliptical tube, there is $\sin 2\varphi$ on the second term in parameter B, so pressure gradient becomes negative if φ is greater than 90 deg, which obstacles to the discharge of liquid film, yet accelerates the separation. Only if e is great enough can parameter B be negative, leading to the separation of liquid film, as shown in Fig. 8(*a*). For an equiangular spiral tube, $\sin\varphi$ becomes negative after θ exceeds certain value. If m is great enough, parameter B can also become negative, resulting in the separation of liquid film, as shown in Fig. 8(*b*). These explain the reason why liquid film separates and for tubes with the same geometry, the separating area increases with the curvature increased if liquid separates.

8 Model Validation

The average heat transfer coefficient for the circular tube from present model are compared with the numerical data from Tang et al. [11], and the deviation is within ±25%, as shown in Fig. 9. There are two reasons that may explain the discrepancies in heat transfer data. On one hand, values of physical parameters are different. On the other hand, numerical calculation in itself has a certain discrepancy.

9 Conclusions

(1) A generalized mathematical model of gas film thickness, liquid film thickness and heat transfer coefficient, and its program have been developed for laminar film condensation in the presence of a noncondensable gas on a horizontal tube with different geometries, including the circular tube, the elliptical tube, and the equiangular spiral tube.
(2) For tubes with the same geometry, gas film thickness, and liquid film thickness near the top of the tube decrease with the increasing of the curvature, and the overall heat transfer rate increases with the curvature increased. The overall heat transfer rate of both an elliptical tube and an equiangular spiral tube are greater than that of a circular one.
(3) For tubes with different geometries, one need to take into account all factors to compare their overall heat transfer rate like gas film thickness, liquid film thickness and the separating area. The decreasing sequence of the overall heat transfer rate is as $m=2.0>m=1.0>e=0.9>m=0.3>e=0.8>m=0.1>e=0.6>$ circular.
(4) This study analyzes the mechanism of the influence of tube geometry and curvature on the drainage and separation of gas film and liquid film. For free convection, gas film never separate because parameter A is always positive, whereas liquid film can separate if parameter B becomes negative.

Nomenclature

a = thermal diffusion coefficient (m^2 s^{-1})
b_1 = half length of major axis for ellipse (m)
b_2 = half length of minor axis for ellipse (m)
c_p = specific heat at constant pressure (J kg^{-1} K^{-1})
D = mass diffusion coefficient (m^2 s^{-1})
D_e = equivalent diameter (m)
e = eccentricity of ellipse ($=(b_1{}^2-b_2{}^2)^{0.5}/b_1$)
g = acceleration of gravity (N kg^{-1})
h = local heat transfer coefficient (W K^{-1} m^{-2})
h_{fg} = latent heat (J kg^{-1})
h'_{fg} = latent heat modified considering subcooling (J kg^{-1}) ($=h_{fg}+3/8c_{pl}(T_i-T_w)$)
k = thermal conductivity (W m^{-1} K^{-1})
ι = half of the tube perimeter (m)
Le = Lewis number ($=a/D$)
m = parametric constant of polar curve
M = molar mass (kg kmol^{-1})
m_c = condensate mass flux (kg m^{-2} s^{-1})
p = pressure (Pa)
q_s = heat flux (W m^{-2})
Sc = Schmidt number ($=v/D$)
T = temperature (K)
u = velocity component in x-direction (m s^{-1})
v = velocity component in y-direction (m s^{-1})
w = mass fraction
x = tangential direction along the tube surface (m)
y = normal direction at any point to the tube surface (m)

Greek Symbols

β = angle between chord OB and horizontal direction (rad)
δ = boundary layer thickness (m)
θ = angle measured from top of tube (rad)
μ = dynamic viscosity (kg m^{-1} s^{-1})
υ = kinematic viscosity (m^2 s^{-1})
ρ = mass density (kg m^{-3})
σ = surface tension coefficient (N m^{-1})
φ = angle between tangent to tube surface and horizontal direction (rad)

Subscripts

av = average
b = bulk
i = gas–liquid interface
l = liquid film
m = gas film or boundary layer of noncondensable gas diffusion
nc = noncondensable gas
t = boundary layer of mixture heat transfer
u = boundary layer of mixture momentum
v = vapor
w = tube surface
0 = the value at the previous iteration

References

[1] Yang, S. A., and Hsu, C. H., 1997, "Free- and Forced-Convection Film Condensation From a Horizontal Elliptic Tube With a Vertical Plate and Horizontal Tube as Special Cases," Int. J. Heat Fluid Flow, **18**(6), pp. 567–574.

Downloaded From: https://thermalscienceapplication.asmedigitalcollection.asme.org on 06/29/2019 Terms of Use: http://www.asme.org/about-asme/terms-of-use

[2] Memory, S. B., Adams, V. H., and Marto, P. J., 2009, "Free and Forced Convection Laminar Film Condensation on Horizontal Elliptical Tubes," Int. J. Heat Mass Transfer, **40**(14), pp. 3395–3406.
[3] Chang, T. B., and Yeh, W. Y., 2011, "Theoretical Investigation Into Condensation Heat Transfer on Horizontal Elliptical Tube in Stationary Saturated Vapor With Wall Suction," Appl. Therm. Eng., **31**(5), pp. 946–953.
[4] Li, H. J., 2009, "Experimental Study on the Performance of Condensation Heat Transfer With Drop-Shaped Tubes," Proc. CSEE, **29**, pp. 79–84.
[5] Som, S. K., and Chakraborty, S., 2006, "Film Condensation in Presence of Noncondensable Gases Over Horizontal Tubes With Progressively Increasing Radius of Curvature in the Direction of Gravity," Int. J. Heat Mass Transfer, **49**(3–4), pp. 594–600.
[6] Mukhopadhyay, S., Som, S. K., and Chakraborty, S., 2007, "A Generalized Mathematical Description for Comparative Assessment of Various Horizontal Polar Tube Geometries With Regard to External Film Condensation in Presence of Noncondensable Gases," Int. J. Heat Mass Transfer, **50**(17–18), pp. 3437–3446.
[7] Yang, S. M., and Tao, W. Q., 2006, *Heat Transfer*, 4th ed., Higher Education Press, Beijing, China.
[8] Lee, K. Y., and Kim, M. H., 2008, "Effect of an Interfacial Shear Stress on Steam Condensation in the Presence of a Noncondensable Gas in a Vertical Tube," Int. J. Heat Mass Transfer, **51**(21–22), pp. 5333–5343.
[9] Rosa, J. C., Herranz, L. E., and Munoz-Cobo, J. L., 2009, "Analysis of the Suction Effect on the Mass Transfer When Using the Heat and Mass Transfer Analogy," Nucl. Eng. Des., **239**(10), pp. 2042–2055.
[10] Hsu, C. H., and Yang, S. A., 1999, "Pressure Gradient and Variable Wall Temperature Effects During Filmwise Condensation From Downward Flowing Vapors Onto a Horizontal Tube," Int. J. Heat Mass Transfer, **42**(13), pp. 2419–2426.
[11] Tang, G. H., Hu, H. W., Zhuang, Z. N., and Tao, W. Q., 2012, "Film Condensation Heat Transfer on a Horizontal Tube in Presence of a Noncondensable Gas," Appl. Therm. Eng., **36**, pp. 414–425.

Downloaded From: https://thermalscienceapplication.asmedigitalcollection.asme.org on 06/29/2019 Terms of Use: http://www.asme.org/about-asme/terms-of-use